Active maintenance of nuclear actin by importin 9 supports transcription

Joseph Dopie[a,1], Kari-Pekka Skarp[a,1], Eeva Kaisa Rajakylä[a], Kimmo Tanhuanpää[b], and Maria K. Vartiainen[a,2]

[a]Program in Cell and Molecular Biology and [b]Light Microscopy Unit, Institute of Biotechnology, University of Helsinki, 00014 Helsinki, Finland

Edited by Larry Gerace, The Scripps Research Institute, La Jolla, CA, and accepted by the Editorial Board January 4, 2012 (received for review November 17, 2011)

Besides its essential and well established role as a component of the cytoskeleton, actin is also present in the cell nucleus, where it has been linked to many processes that control gene expression. For example, nuclear actin regulates the activity of specific transcription factors, associates with all three RNA polymerases, and is a component of many chromatin remodelling complexes. Despite the fact that two export receptors, Crm1 and exportin 6, have been linked to nuclear export of actin, the mechanism by which actin enters the nucleus to elicit these essential functions has not been determined. It is also unclear whether actin is actively exchanged between the nucleus and the cytoplasm, and whether this connection has any functional significance for the cell. By applying a variety of live-cell imaging techniques we revealed that actin constantly shuttles in and out of the nucleus. The fast transport rates, which depend on the availability of actin monomers, suggest an active transport mechanism in both directions. Importantly, we identified importin 9 as the nuclear import factor for actin. Furthermore, our RNAi experiments showed that the active maintenance of nuclear actin levels by importin 9 is required for maximal transcriptional activity. Measurements of nuclear export rates and depletion studies also clarified that nuclear export of actin is mediated by exportin 6, and not by Crm1. These results demonstrate that cytoplasmic and nuclear actin pools are dynamically connected and identify the nuclear import and export mechanisms of actin.

Recent studies have shown that the cell nucleus is highly compartmentalized. Both the genome itself, and its associated processes, such as transcription, are nonrandomly distributed within the nucleus. This organization is extremely dynamic and has been reported to vary, for example, upon cell differentiation and also in certain diseases, including cancer. The compartmentalization has a profound impact on nuclear functions and therefore plays a critical role in controlling gene expression (1). Despite these essential tasks, the molecular mechanisms driving nuclear organization are poorly understood. An excellent candidate for mediating this process is actin, the traditional component of the cytoplasmic cytoskeleton.

Actin has both the necessary nuclear connections and the biochemical properties required to act as the master organizer of nuclear structure and function. Actin is a component of many chromatin remodelling complexes (2, 3), associates with all three RNA polymerases (4–6), and also binds to factors regulating pre-mRNA processing and export (7–9). In addition to these general roles in gene expression, actin has also been linked to regulation of specific sets of genes. For example, nuclear actin regulates the localization and activity of myocardin-related transcription factor A (MRTF-A), which is a coactivator of the transcription factor serum response factor (SRF) (10), and abrogates the basal repression of Toll-like receptor-responsive genes through a mechanism involving coronin 2a, which is an actin filament-binding protein (11). Actin therefore has links to protein complexes that span the whole regulatory spectrum of the gene expression process. The most fundamental biochemical property of actin is its ability to produce force, either through polymerization or in conjunction with motor protein myosins. In the cytoplasm, these processes are harnessed for instance during cell migration to push the plasma membrane forward (12) or for muscle contraction (13), respectively. It is therefore plausible that these biochemical properties of actin are utilized also within the nucleus. Indeed, actin and nuclear myosins have been implicated in the movement of individual gene loci upon transcription activation (14–16) and even in rearranging whole chromosomes within the nucleus (17). Furthermore, although the functional conformation of nuclear actin is still under debate (18, 19), many of the nuclear actin related functions mentioned above are disrupted upon treatment of cells with drugs affecting actin polymerization (15, 20, 21), suggesting that actin polymerization plays a role also in the cell nucleus.

If actin acts as master organizer within the nucleus, it is conceivable that changes in nuclear actin amounts and/or polymerization properties would have an immense impact on nuclear functions and could therefore be used to elicit profound changes in gene expression to drive different cellular fates. In support of this it was recently discovered that extracellular cues induce a reduction in nuclear β-actin levels resulting in cell quiescence (22). In another example, treating HL-60 cells with phorbol 12-myristate 13-acetate, which induces their differentiation, resulted in approximately 30-fold increase in levels of nuclear actin, demonstrating a dramatic shift in the cellular actin balance (23). Also amphibian oocytes, which contain massive amounts of actin in their nuclei (24), require nuclear actin polymerization for transcriptional reprogramming (21). Therefore, it is reasonable to assume that the cell has devised strategies to achieve and maintain the required balance between cytoplasmic and nuclear actin pools.

The mechanism of actin entry into the nucleus is not known but two export pathways have been reported. It has been suggested that treating cells with leptomycin B (LMB), a selective inhibitor of Crm1 (exportin 1) (25), results in the nuclear accumulation of actin and that actin would contain nuclear export signal (NES) sequences (26). However, another study found no evidence of Crm1 recognizing actin as an export cargo, whereas depleting exportin 6 (Exp6) with RNAi resulted in distinct nuclear actin bars in *Drosophila* cells. Moreover, pull-down assays with Exp6 specifically showed binding to actin and profilin (27). These data suggest that the active regulation of nucleo-cytoplasmic actin balance takes place at least at the level of export.

Here, we have used different microscopy techniques to study nuclear actin dynamics, and show that actin constantly shuttles between the cytoplasm and the nucleus. We clarify the ambiguous reports on nuclear export of actin and show that Exp6, not Crm1, is responsible for the export of actin from the nucleus. Second, our microscopy data suggested an active import mechanism for

Author contributions: M.K.V. designed research; J.D., K.-P.S., E.K.R., and M.K.V. performed research; M.K.V. contributed new reagents/analytic tools; J.D., K.-P.S., E.K.R., K.T., and M.K.V. analyzed data; and J.D., K.-P.S., and M.K.V. wrote the paper.

The authors declare no conflict of interest.

This article is a PNAS Direct Submission. L.G. is a guest editor invited by the Editorial Board.

Freely available online through the PNAS open access option.

[1]J.D. and K-P.S. contributed equally to this work.

[2]To whom correspondence should be addressed. E-mail: maria.vartiainen@helsinki.fi.

See Author Summary on page 3205 (volume 109, number 9).

This article contains supporting information online at www.pnas.org/lookup/suppl/doi:10.1073/pnas.1118880109/-/DCSupplemental.

actin and we confirm this with RNAi experiments on known components of the active transport machinery and identify cofilin and importin 9 (Ipo9) as mediators of nuclear localization of actin. Finally, we demonstrate that the active nuclear localization of actin is required to maintain the appropriate levels of actin in the nucleus, which are required for maximal transcription.

Results

Nuclear Export of Actin Is Mediated by Exp6 and Is Not Sensitive to Crm1 Inhibition. Actin has many important roles both in the cytoplasm and in the nucleus, yet it is not well known how these two actin pools are connected. All transport between these two compartments takes place through nuclear pore complexes (NPCs). This channel allows passive diffusion of small molecules, whereas larger molecules need to be actively transported in an energy-dependent manner by importin/exportin proteins (28). The size limit of passive diffusion was reported to be around 40 kDa or 45 Å (29, 30), and because the size of actin, 42 kDa [3.3 × 5.5 nm (31)], it has been unclear whether actin uses a passive or an active mechanism to enter the nucleus.

To investigate how actin travels between the nucleus and the cytoplasm we used different photobleaching assays in cells expressing GFP-actin either stably or through transient transfection, and in cells microinjected with fluorescently labeled actin. To study the dynamics of nuclear export of actin we used fluorescence loss in photobleaching (FLIP), where we repeatedly bleach the cytoplasm and follow the loss of nuclear fluorescence, which is due to fluorescent molecules being exported out of the nucleus and then bleached in the cytoplasm (Fig. 1*A*). In GFP-actin expressing cells, the nuclear fluorescence was rapidly and efficiently decreased upon cytoplasmic bleaching, demonstrating that actin is constantly being exported out of the nucleus (Fig. 1*B* and Fig. S1*A*). Cytoplasmic bleaching did not significantly decrease the nuclear fluorescence of RanBP1-GFP with a deleted nuclear export signal nor that of MRTF-A-GFP, a known export cargo of Crm1 (10) confined to the nucleus with a specific inhibitor, LMB (25) (Fig. 1*B*). To directly test the involvement of Crm1 in nuclear export of actin, cells were treated with LMB for 30–60 min. This treatment did not decrease the nuclear export rates of GFP-actin (Fig. 1*B*). In fact, the export rates for GFP-actin slightly increased whereas no effect with LMB was seen for GFP-actin-R62D, which is an actin mutant that does not polymerize (32). Also, there was no difference in the distribution of GFP-actin between the nucleus and the cytoplasm in LMB-treated cells (Fig. 1*C*). LMB treatment efficiently inhibited Crm1 as MRTF-A accumulated in the nucleus (Fig. 1*C*). Interestingly, GFP-actin-R62D was exported faster from the nucleus compared to wild-type GFP-actin (Fig. 1*B*), suggesting that the availability of actin monomers limits the nuclear export rates. Importantly, we were never able to completely bleach actin out of the nucleus during this FLIP experiment (Fig. S1*A*) or even upon longer bleaching, suggesting that a fraction of actin is associated with nuclear complexes in a more stable fashion.

To further explore the roles of Crm1 and Exp6 in nuclear export of actin, we used RNAi in both mammalian and *Drosophila* S2R+ cells. Depletion of Crm1 in either mouse fibroblasts stably expressing GFP-actin (Fig. 1*D*) or in *Drosophila* cells (Fig. 1 *E* and *F*) did not result in nuclear accumulation of actin. Crm1 depletion was efficient as MRTF-A-GFP was present in the nucleus of these cells (Fig. S1*B*). However, depletion of Exp6 in mouse fibroblasts resulted in clear accumulation of GFP-actin in the nucleus (Fig. 1*D*), supporting an earlier observation in human diploid fibroblasts (33). In *Drosophila* S2R+ cells, depletion of Exp6 also accumulated actin in the nucleus, and the phenotype manifested as a phalloidin-stainable bar in about 50% of the cells (Fig. 1 *E* and *F*), as also shown previously in S2 cells (27). Confocal microscopy was used to confirm the nuclear localization of this bar (Fig. S1*C*). Of note, in mammalian cells we never observed formation of a phalloidin-stainable bar in the cell nucleus upon Exp6 depletion, as also shown previously (34). Taken together, we show that actin is constantly exported out of the nucleus, demonstrate that this process is likely mediated by Exp6, and that Crm1 does not play a role in nuclear export of actin.

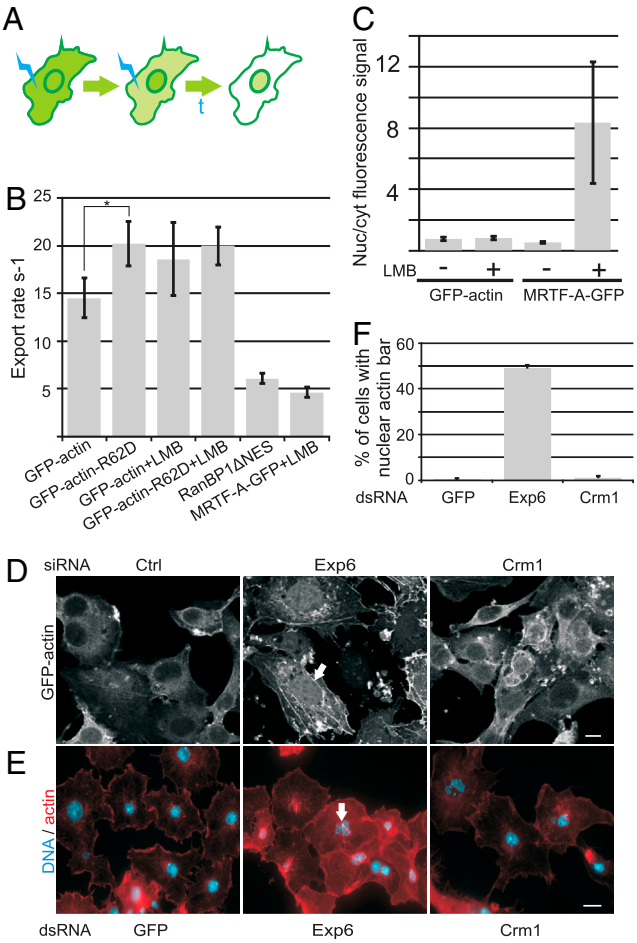

Fig. 1. Actin is constantly exported out of the nucleus, and the export is not sensitive to Crm1 inhibition. (*A*) Schematic of the FLIP assay to measure actin export by continuous bleaching of the cytoplasm. (*B*) Nuclear export rate quantified from the first four data points of FLIP-curves; data represent mean rates from individual experiments +/− std ($n = 7$–10). Asterisk indicates $P = 0.014$. (*C*) Ratio of nuclear and cytoplasmic (nuc/cyt) fluorescence intensities of GFP-actin and MRTF-A-GFP, with and without LMB. Data represent mean fluorescent intensity signal ratios +/− std ($n = 10$–25). (*D*) Confocal microscopy images of GFP-actin expressing NIH 3T3 cells transfected with negative control, Crm1, or Exp6 siRNAs. Arrow indicates nuclear GFP-actin accumulation. (*E*) Fluorescence microscopy images showing the distribution of actin filaments by phalloidin staining (red) in control (Ctrl), Crm1, and Exp6 dsRNA treated *Drosophila* S2R+ cells. DAPI; cyan. Arrow indicates actin bar in the nucleus of Exp6-depleted cells. Scale bars, 10 μm. (*F*) Quantification of the percentage of cells with nuclear actin bars in *E* for two independent experiments +/− std ($n = 200$ cells per treatment).

Nuclear Import of Actin Is an Active Process. To understand how actin is imported into the nucleus, we used a fluorescence recovery after photobleaching (FRAP) assay to measure the import rates of fluorescently tagged constructs. In the assay, the whole nucleus is bleached void of fluorescence and the initial recovery, which is the result of the import of unbleached molecules from the cytoplasm, is used as a measure of import (Fig. 2 *A* and *B*). Both GFP-tagged β-actin and Alexa-Fluor-488-tagged α-actin recovered their nuclear fluorescence at similar rates, illustrating the continuous input of these two actin isoforms into the nucleus (Fig. 2*C*). This together with the data on actin export (Fig. 1*C*) shows that actin constantly shuttles in and out of the nucleus in living cells. In

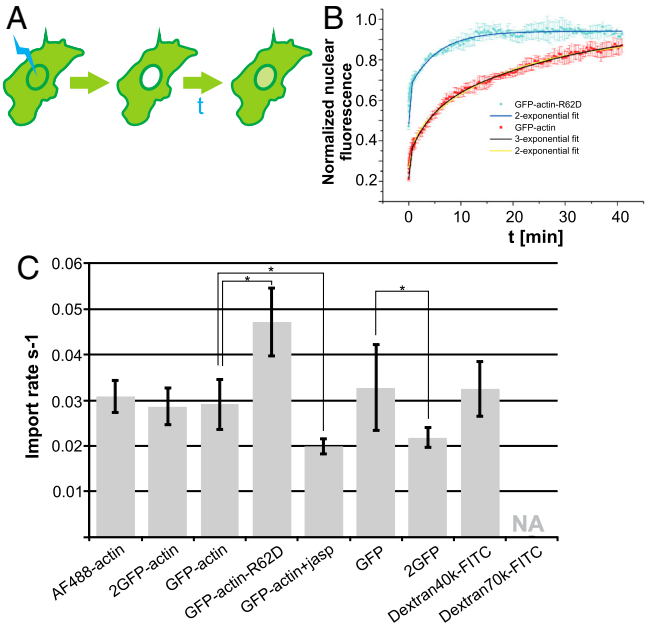

Fig. 2. Nuclear import of actin is an active process. (*A*) Schematic of the FRAP assay to measure actin import by bleaching the nucleus. (*B*) A longer FRAP experiment with GFP-actin and R62D mutant; data represent mean nuclear fluorescence intensity +/− std ($n = 5$). Fitted (either 2- or 3-exponential) curves are shown on top of the raw data. (*C*) Nuclear import rate quantitated from the first 12 data points of shorter 1 min FRAP curves; data represent mean rates from individual experiments +/− std ($n = 6$–11). Asterisks indicate $P = 0.012$ (GFP-actin vs. GFP-actin-R62D), $P = 0.022$ (GFP-actin vs. GFP-actin+jasp), $P = 0.043$ (GFP vs. 2GFP). For this experiment, cells were either transfected or microinjected [Alexa Fluor (AF) 488-actin, dextrans]. Jasp, 100 nM jasplakinolide.

agreement with the data on actin export, unpolymerizable GFP-actin-R62D was imported faster into the nucleus than the wild-type GFP-actin, highlighting again the importance of the availability of transport competent actin monomers. Accordingly, prodding the actin monomer/polymer balance towards F-actin with jasplakinolide appeared to have a limiting effect on nuclear import (Fig. 2*C*).

When comparing the import rate of GFP-actin to passively travelling constructs like 40 kDa dextran, the much larger actin construct travels at a similar rate (Fig. 2*C*), whereas the import rate of 70 kDa dextran could no longer be effectively measured with our assay due to the fact that it is mostly excluded from the nucleus. The size of GFP-actin, 69 kDa, positions the chimera well beyond the nuclear pore complex exclusion limit suggesting that an active component might play a role in the import of actin. This hypothesis is further confirmed by the fact that increasing the size of the construct to almost 100 kDa by fusing another GFP to GFP-actin, 2GFP-actin still retains the fast import rate observed for GFP-actin (Fig. 2*C*). Also, the distribution between nucleus and cytoplasm was similar for the three actin constructs (Fig. S1*D*). In contrast, the import rate of 2GFP was significantly slower than that of GFP (Fig. 2*C*), demonstrating that passive diffusion is sensitive to the size of the construct, and because this phenomenon was not observed for actin, this finding further suggests an active import pathway for this protein.

We also performed longer FRAP experiments and observed the recovery of nuclear fluorescence for 42 min in cells transfected with GFP-actin or GFP-actin-R62D. Interestingly, three phases of recovery can be witnessed with the wild-type actin whereas the recovery of the R62D mutant is limited to two phases (Fig. 2*B* and *Material and Methods* for details). The first phase with the shortest half life of 7 s is likely to correspond to the rapidly moving actin monomers because it is present for both constructs. For GFP-actin, the half life of the second phase is 230 s and it corresponds in amplitude to the polymeric phase witnessed previously (20). The half life of the longest phase in the wild-type curve was 1,800 s, and thus demonstrates that a substantial population of actin (approximately 60%) is relatively tightly associated with nuclear complexes, and is relatively slowly exchanged from them. This same pool was also evident in the export assay (Fig. S1*A*). The other phase of the R62D mutant has a half life of 330 s. Because the construct is unable to polymerize, this pool is also likely to represent binding to nuclear structures, although the mutant may not be able to enter all the complexes the wild type can. To summarize, our FRAP experiments demonstrate that actin likely uses an active mechanism to enter the nucleus, and that in addition to the monomeric and polymeric pools, a substantial population of nuclear actin is also found tightly associated within nuclear complexes.

Ran-Gradient and Cofilin Are Required for Nuclear Import of Actin. Functional RanGTP/RanGDP-gradient between the nucleus and the cytoplasm as well as importin/exportin proteins are required for all active, i.e., energy-consuming nuclear import and export processes (28). Therefore, we wanted to examine whether nuclear import of actin is also dependent on these factors. To more easily visualize actin in the nucleus, we took advantage of the fact that upon Exp6 depletion in *Drosophila* S2R+ cells actin accumulates in the nucleus and forms a phalloidin-stainable bar, which is easy to visualize and score under the microscope (Fig. 1*E*; Fig. 3 *A* and *B*, Fig. S1*C*). We then screened all identified *Drosophila* nuclear transport factors for their ability to rescue the Exp6 phenotype. Supporting our imaging data, we found that Ran-depleted cells failed to accumulate actin in the nuclei in the absence of actin export (Fig. 3 *A* and *B*), suggesting that the Ran-gradient is required for nuclear accumulation of actin. This also supports the notion that the process is active, although we cannot

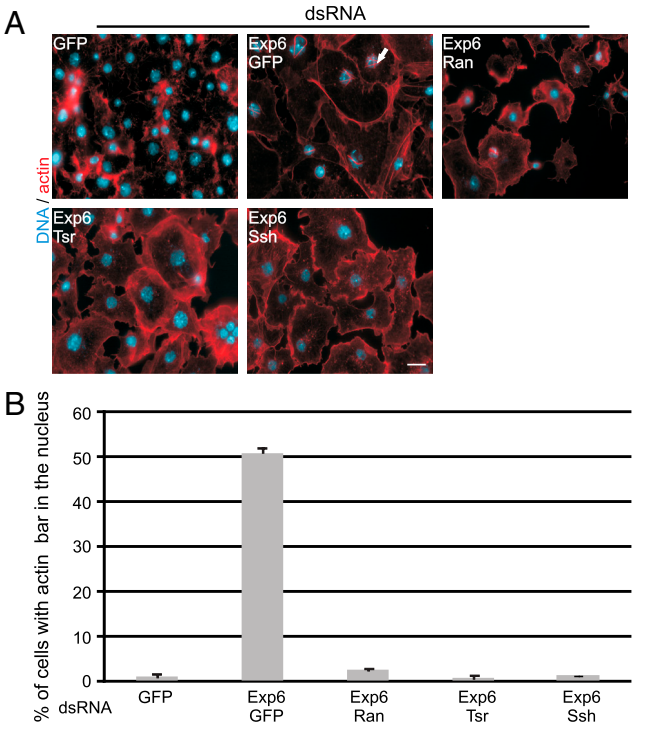

Fig. 3. Dephosphorylated cofilin is required for nuclear localization of actin. (*A*) Fluorescence microscopy images of *Drosophila* S2R+ cells after dsRNA treatment as indicated. DsRNA against GFP is used as a negative control. Arrow indicates actin bar in the nucleus. Phalloidin (red); DAPI (cyan). Scale bars, 10 μm. (*B*) Quantification of the percentage of cells in two independent experiments with nuclear actin bars +/− std ($n = 200$ cells per treatment). Tsr, Twinstar (*Drosophila* cofilin); Ssh., Slingshot.

rule out unspecific effects of Ran depletion. Nevertheless, depletion of Ran did not affect passive diffusion, because GFP was localized normally in Ran-depleted cells (Fig. S1*E*). However, none of the import receptors tested in *Drosophila* cells rescued the Exp6-depleted phenotype (Fig. S1*F*).

Actin dynamics are highly regulated in the cytoplasm by various actin binding proteins (ABPs), and because many of them have been localized to the nucleus (19), we postulated that some of these proteins could play a role in the nuclear localization of actin. Because cofilin has been implicated in stress-induced nuclear accumulation of actin (35), we thus tested if cofilin would also be involved in steady-state actin import. Silencing of cofilin (Tsr in *Drosophila*) or slingshot (Ssh), a cofilin phosphatase (36), prevented the formation of the nuclear actin bar caused by Exp6 depletion in *Drosophila* cells (Fig. 3 *A* and *B*). To test the role of cofilin in mammalian cells, we codepleted Exp6 and cofilin-1, which is the major actin-depolymerization factor/cofilin family member in the NIH 3T3 cells used here (37, 38). Cofilin-1 depletion effectively abolished the nuclear accumulation of actin caused by Exp6 silencing (Fig. 4 *A* and *B*) suggesting that the role of cofilin is conserved. To address whether cofilin regulates nuclear import by affecting the actin monomer pool (39), we used NIH 3T3 cells stably expressing the unpolymerizable actin mutant GFP-actin-R62D. The nuclear localization of this mutant was cofilin-dependent (Fig. 4*C*), suggesting that the inability of actin to accumulate in the nucleus when both cofilin and Exp6 are silenced is at least partly due to the absence of import, not merely due to decreased actin monomer levels.

Ipo9 Is Required for the Maintenance of Nuclear Actin Levels. Our RNAi studies supported the direct involvement of cofilin in the nuclear import of actin, but how cofilin is connected to the nuclear import machinery has not been characterized. Although we did not find any *Drosophila* import receptor, depletion of which would have rescued the Exp6 phenotype, we decided to perform a similar screen in mammalian cells. All identified mouse nuclear import factors were targeted and assessed for their ability to rescue the Exp6 depletion induced nuclear accumulation of GFP-actin. The only import receptor that was capable of reversing the nuclear accumulation of actin was Ipo9 (Fig. 4*A*), a member of the importin-β superfamily. Furthermore, expressing RNAi-resistant Ipo9 construct (Fig. S2 *A* and *B*) in Ipo9- and Exp6-depleted cells restored the nuclear accumulation of actin (Fig. 4*B*). Codepletion of Ipo9 with Exp6 did not affect the depletion of Exp6 protein

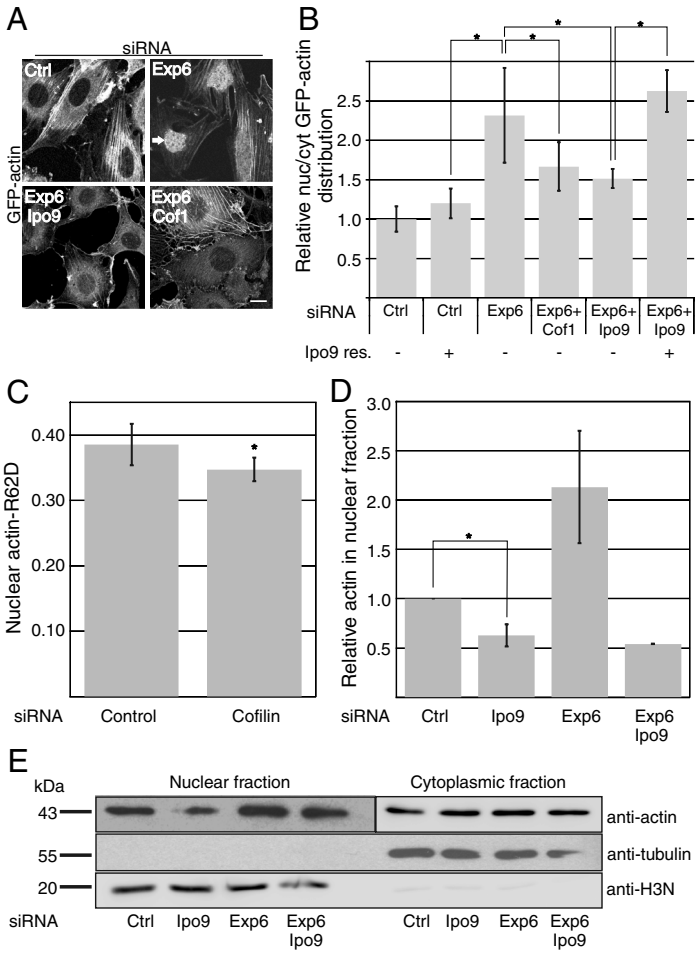

Fig. 4. Ipo9 is required for the maintenance of nuclear actin levels. (*A*) Confocal microscopy images of GFP-actin expressing mammalian cell line transfected with siRNAs as indicated. Arrow indicates increased GFP-actin in the nuclei of Exp6-depleted cells. (*B*) Relative ratio of nuclear (nuc) and cytoplasmic (cyt) GFP-actin fluorescence intensities quantified. Data represent mean fluorescent intensity signal ratios +/− std from three individual experiments ($n = 21$–154 cells per treatment) and are normalized to control siRNA-transfected cells. Asterisks indicate $P = 9.2E\text{-}27$ (Ctrl vs. Exp6), $P = 3.9E\text{-}12$ (Exp6 vs. Exp6+Ipo9), $P = 1.3E\text{-}08$ (Exp6 vs. Exp6+Cof1), $P = 1.8E\text{-}09$ (Exp6+Ipo9 vs. Exp6+Ipo9+Ipo9res). (*C*) Nuclear GFP-actin-R62D in control and cofilin siRNA-treated cells. Data represent mean fluorescent intensity signal ratios +/− std from three independent experiments with $n = 17$–19. Asterisk indicates $P = 0.032$. (*D*) Quantification of relative amounts of actin in the nuclear fraction. Data represent mean +/− std from three independent experiments and are normalized to control siRNA. Asterisk indicates $P = 0.018$ [Control (Ctrl) vs. Ipo9]. (*E*) Western blots analysis of nuclear and cytoplasmic protein fractions from siRNA-treated cells detected with the indicated antibodies.

(Fig. S2*C*). Next, we took nuclear fractions after RNAi-mediated depletion of export and/or import receptors and assessed the levels of endogenous nuclear actin. The amount of nuclear actin in Ipo9-depleted cells was dramatically reduced (Fig. 4 *D* and *E*; Fig. S2 *D* and *E*) signifying the requirement of this receptor in the active maintenance of nuclear actin levels. This finding prompted us to ask why we failed to identify Ipo9 in *Drosophila* cells. Further investigation revealed that the *Drosophila* ortholog of Ipo9 is surprisingly stable and even after 5 d of RNAi, the protein level was not significantly depleted (Fig. S2*F*). Importantly, both cofilin and actin interact with Ipo9 in a coimmunoprecipitation experiment (Fig. 5 *A* and *B*). Cofilin seemed to be required for the interaction between actin and Ipo9, because decreasing the amount of cofilin in the immunoprecipitation reaction concomitantly decreased association between actin and Ipo9 (Fig. 5*A*). Significantly, the interaction between cofilin and Ipo9 could be disrupted by the addition of Ran-Q69L (Fig. 5*B*), which is a mutant that traps Ran in its GTP bound form (40), thus mimicking nuclear environment. Therefore, the association between cofilin and Ipo9 appears to be a classical importin-cargo interaction (41).

Active Nuclear Localization of Actin Supports Transcription. To test if reduced nuclear actin levels achieved by Ipo9 depletion have functional consequences for the cells, we analyzed 5-fluorouridine (5-FUrd) incorporation into nascent mRNA. We observed that 5-FUrd incorporation was significantly reduced in Ipo9-depleted cells (Fig. 6 *A* and *B*). Transfection of the Ipo9-depleted cells with an RNAi-resistant Ipo9 construct (Fig. S2 *A* and *B*) efficiently rescued the transcription (Fig. 6*B*), proving that the Ipo9 siRNA was specific. Also cofilin-depleted cells showed reduced 5-FUrd incorporation as compared to control cells (Fig. 6*B*), as demonstrated previously (42). Interestingly, excess nuclear actin promoted by Exp6 depletion would slightly hinder transcription (Fig. 6*B*), which might be an indirect consequence of cytoplasmic defects, because the actin cytoskeleton was often disorganized in the Exp6 depleted cells (Fig. 1*E*). To assess, whether the reduced transcription in Ipo9-depleted cells is specifically due to decreased nuclear actin, we created a cell line expressing Flag-NLS-actin, which contains the SV40 nuclear localization signal (NLS), which is capable of delivering actin into the nucleus via the importin-α/β route upon repression of Ipo9-dependent actin import. Importantly, Ipo9 depletion fails to decrease transcription in this cell line (Fig. 6*C*), thus proving the nuclear actin-specific effect. However, the lack of cofilin 1 in this cell line has a measurable impact on transcription (Fig. 6*C*), corroborating earlier findings that cofilin might play a direct role in RNA-polymerase-II-mediated transcription (42).

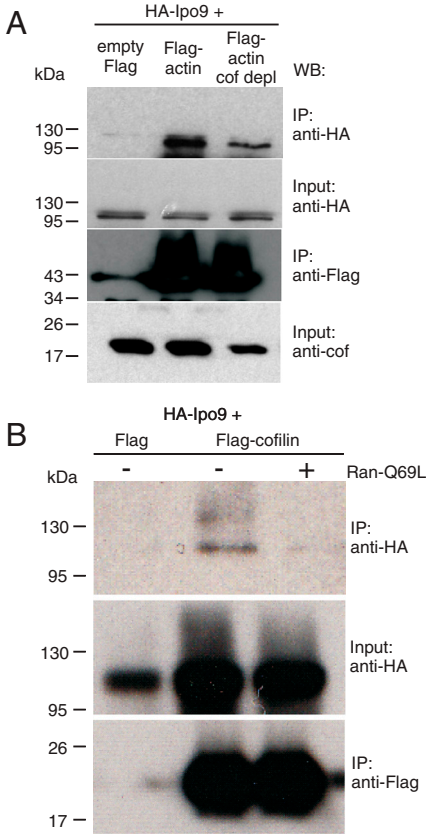

Fig. 5. Ipo9 interacts with actin and cofilin. (*A*) Western blots with HA/Flag antibodies of coimmunoprecipitation assay using Flag-antibodies with HA-Ipo9 and indicated Flag constructs. Cofilin was immunodepleted prior to the coimmunoprecipitation in the cofilin depleted (cof depl) sample. (*B*) Western blots with HA/Flag antibodies of coimmunoprecipitation assay using Flag antibodies with HA-Ipo9 and indicated Flag constructs with and without addition of Ran-Q69L. IP, immunoprecipitation sample.

Discussion

The eukaryotic cell has confined significant functions to the nucleus but this confinement is in balance and dependent on carefully regulated transport of selected components via almost two dozen export/import receptors, which bind to different cargo molecules and pass through NPCs. In this study, we show that in interphase cells actin, a potential master regulator of nuclear structure and function, continuously shuttles between the nucleus and the cytoplasm and that this process requires components of the active translocation machinery both during entrance and exit. It is also significant that actin seems to travel together with small ABPs; cofilin on the way in and profilin on the way out (27). This may not only be crucial for maintaining nuclear actin levels, but also to actively balance the distribution of these filament severing/promoting factors and may explain the distinct properties of the cytoplasmic and nuclear actin networks. Besides identifying the molecular players involved in nucleo-cytoplasmic shuttling of actin, we also provide evidence that these factors are critical regulators of the transcriptional activity of the cell through their ability to modulate nuclear actin levels. This further strengthens the notion that nuclear actin plays an important role in the functional organization of the nucleus.

Our data pin the primary role in the nuclear export of actin to Exp6. This is in contrast to an earlier report implicating Crm1 in actin export (26). Our direct measurements of nuclear export rates of actin (Fig. 1*B*) at conditions where Crm1 is already efficiently inhibited demonstrate that nuclear export of actin is not acutely decreased by Crm1 inhibition. An observation of increased nuclear actin levels after prolonged LMB treatment could, for instance, be explained by the general requirement for Crm1 in many export processes. Indeed, Crm1 is utilized by many ABPs, such as MRTF-A (10), and the blockage of this pathway is therefore bound to increase binding sites for actin in the nucleus, thus potentially increasing nuclear actin levels with time. Nuclear accumulation of different actin-regulators, which keep actin in export-competent monomeric form, may also explain our finding that nuclear export of actin in fact seems slightly faster in LMB-treated cells than in control cells. This idea is supported by the observation that LMB did not affect nuclear export of the unpolymerizable actin mutant (Fig. 1*B*).

The nuclear import mechanism of actin has not been previously characterized. The size of actin, which in theory may allow passive diffusion through NPCs, makes the task of discriminating between active and passive transport difficult. Our bleaching experiments demonstrate that increasing the size of the actin construct well beyond the nuclear pore exclusion limit does not decrease the nuclear import rates of actin (Fig. 2*C*), thus pointing to active transport, because passive diffusion would be sensitive

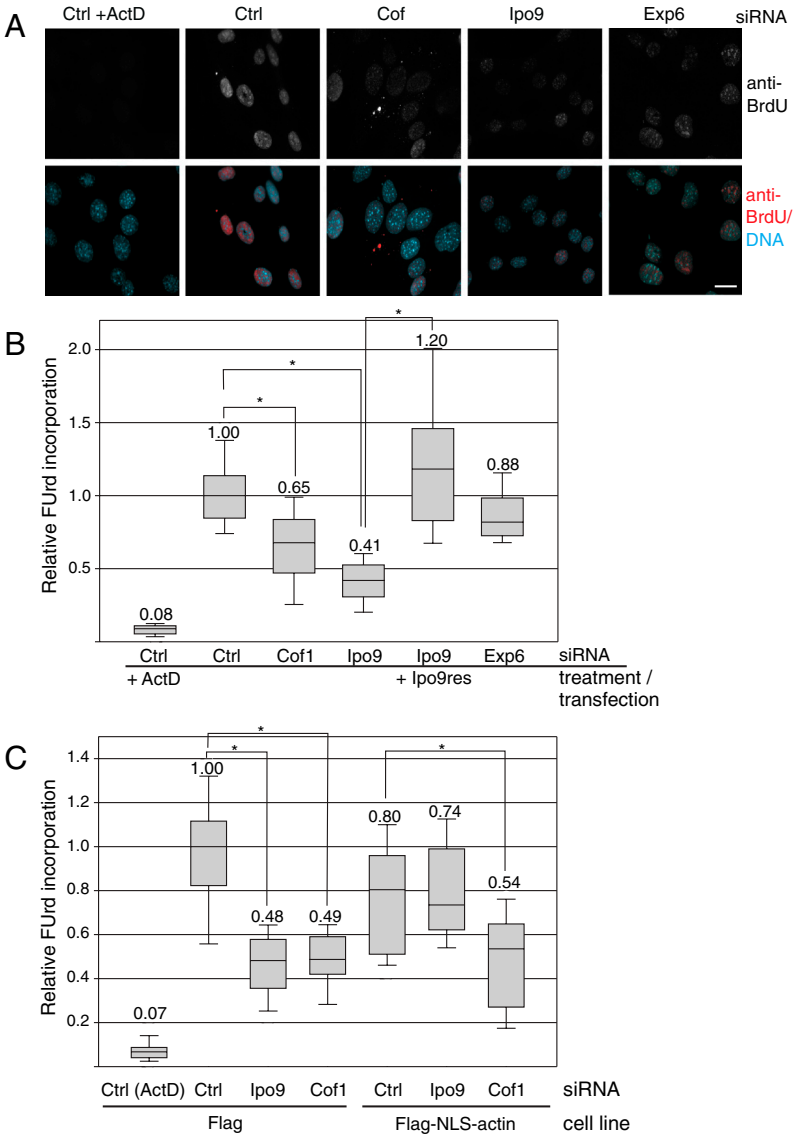

Fig. 6. Active nuclear transport of actin supports transcription. (*A*) Immunofluorescence images of mammalian cells transfected with siRNAs and treated with actinomycin D (ActD) as indicated. 5 FUrd incorporation was used as a measure of transcription and detected with anti-BrdU (*Upper*). *Lower* shows a merged image of anti-BrdU (red), and DAPI (cyan). Scale bar = 10 μm (*B*) Quantification of BrdU signal is shown as box-and-whisker plots with median and 5th/95th percentile for NIH 3T3 cells treated with indicated siRNAs. When indicated the cells were treated with ActD or were expressing the Ipo9 siRNA resistant construct (Ipo9res). Data were normalized to control siRNA. (*C*) Quantification of BrdU signal shown in box-and-whisker plot for cell lines expressing either the empty vector (Flag) or Flag-NLS-actin, and treated with the indicated siRNAs (more than 20 cells were quantified per treatment), and data were normalized to control siRNA in the Flag-cell line. Median value is indicated on top of the whisker and the asterisks indicate $P \leq 0.001$.

to the size of the construct, as shown for GFP and 2GFP import rates (Fig. 2*C*). This conclusion is further supported by the fact that depletion of a specific nuclear transport factor, Ipo9, with RNAi blocked nuclear accumulation of actin (Fig. 4*D*). Actin lacks classical nuclear localization signals. Earlier data have suggested a role for cofilin in actin nuclear accumulation in special situations, such as stress (35). However, here we incriminate cofilin as a crucial regulator of the continuous steady-state actin flow into the nucleus. Although our microscopy experiments suggested that the availability of actin monomers is a limiting factor to the nuclear transport of actin, our results showing that the nuclear localization of an unpolymerizable actin mutant (Fig. 4*C*) is also dependent on cofilin point to a direct role for cofilin in nuclear import of actin. It is therefore tempting to speculate that cofilin would play a similar role in mediating the interaction between actin and the nuclear import receptor, as profilin does with Exp6 during nuclear export (27). Indeed, depletion of cofilin seems to decrease the interaction between actin and Ipo9 (Fig. 5*A*), but further biochemical experiments with purified proteins are required to address this hypothesis. We have so far been unable to reconstitute the active nuclear import process of actin in an in vitro nuclear transport assay, possibly suggesting that other components may still be required. The missing component may either be an additional protein or, for example, a posttranslational modification on any of the involved components. In this regard it is curious that small ubiquitin-like modification of actin has been linked to its nuclear localization (43). Both the nuclear import and export assays revealed continuous transport of actin, demonstrating that there is significant crosstalk between the cytoplasmic and nuclear actin pools. This property can be used to transmit information between these two compartments, for example, by signalling to transcription factors. MRTF-A-SRF pathway is an excellent example of this type of signal transmission (10).

Ipo9-depleted cells showed a clear reduction (Fig. 4 *D* and *E*), but not a complete abolishment of nuclear actin. In addition to incomplete depletion taking place in all RNAi experiments, this may be due to passive diffusion, which still takes place when components of the active transport machinery have been disrupted (Fig. S1*E*). Whether Ipo9 is also required for nuclear localization of actin in *Drosophila* warrants further investigations because the *Drosophila* ortholog turned out to be difficult to deplete with RNAi. Considering the high degree of redundancy in higher eukaryotic systems, it is also possible that other actin import pathways exist alongside with the one characterized here.

Our microscopy data expose a previously uncharacterized, relatively stable pool of actin in the nucleus. This is seen as the remaining fraction in the export assay (Fig. S1*A*) and as a very slowly recovering phase in the longer import assay (Fig. 2*B*). We think this pool corresponds to the great number of nuclear interactions suggested for actin. For example, it appears that actin is a relatively stable component of the RNA polymerase complex, because it is almost impossible to purify without the presence of actin (4–6, 8, 44). Because our export FLIP experiment showed that the availability of actin monomers is limiting nuclear export rates of actin, this also suggests that increased binding of actin to nuclear structures, e.g., upon transcriptional activation, would increase the levels of nuclear actin. Accordingly, transcriptionally quiescent cells have less nuclear actin (22) and differentiating, transcriptionally active macrophages display increased actin in their nuclei (23), supporting the idea that an interesting feedback-loop may exist between nuclear actin levels and transcriptional activity of the cell. Indeed, decreased nuclear actin in Ipo9-depleted cells resulted in reduction on 5-FUrd incorporation into nascent transcripts (Fig. 6*B*). Our data also confirm the earlier FRAP data on nuclear actin (20) and suggests that about 25% of actin is present in some type of polymeric form in the nucleus (Fig. 2*B*).

Silencing of either cofilin or Ipo9 significantly repressed transcription (Fig. 6*B*). Ipo9 has other cargos besides actin, and it has been implicated in the nuclear import of histones (45) and c-Jun (46), but the decreased transcription appears actin dependent as the delivery of actin into the nucleus via another import pathway significantly restored the levels of the nascent mRNA (Fig. 6 *B* and *C*). This study shows directly that specific manipulation of nuclear actin levels has consequences on the transcriptional activity of the cell. This result is important because most prior studies linking actin to transcription have utilized general actin-disrupting drugs (15, 20, 21) or in vitro systems (4). Cofilin-1 silencing has also previously been shown to decrease pol II transcription and a direct role for cofilin in transcription elongation has been suggested (42). Our results support this notion because expression of the Flag-NLS-actin fails to rescue the transcription phenotype in cofilin-depleted cells (Fig. 6*C*), demonstrating that the cofilin phenotype cannot be totally explained by lack of nuclear actin. It remains to be determined how global the actin-dependent transcriptional repression is or whether some genes are affected more than others. The latter seems more plausible, because the lack of nuclear actin has already been shown to regulate the specific fluctuations in gene expression required for the normal function of certain epithelial cells (22) and cellular differentiation specifically accumulates actin on certain promoters (23). In *Drosophila,* the DNA adenine methyltransferase identification technique has revealed that actin is found associated with a special type of euchromatin, which is linked to tissue-specific gene expression (47), further suggesting that actin may have gene-specific effect on transcription.

Our data reveal the critical steps in nucleo-cytoplasmic shuttling of actin and therefore opens possibilities for the regulation of nuclear actin levels, and consequently mechanisms that may affect nuclear organization. First, this can take place by manipulating the levels of transport competent monomeric actin and either polymerized actin or actin bound to large macromolecular complexes, such as those engaged in transcription. Second, the binding affinity to export/import receptors may affect nuclear actin levels. This regulatory step is expanded by the small ABPs, which seem to play a crucial role in making actin transport competent. Finally, the regulation of export/import receptors themselves can easily have the most dramatic influence on nuclear actin levels. This has already been witnessed in the development of *Xenopus laevis* oocytes, where the lack of Exp6 results in high nuclear actin levels, which are required for stabilizing the giant nuclei (24), and for transcriptional reprogramming in these cells (21). In the light of the literature from recent years, which cast a multitude of roles for nuclear actin, our data reveal actin to be a dynamic tool, which can be rapidly deployed to oversee diverse tasks within various microenvironments of the cell, most importantly the nucleus. Because more research is being done in higher organisms showing the involvement of nuclear actin in aforementioned crucial steps of cell fate decisions, it would be of interest to identify signalling pathways mediating these processes.

Materials and Methods

Details of DNA constructs, cell lines, DNA transfections, RNA interference, and primers can be found in Supporting Information

Antibodies. The primary antibodies used in this study include: actin (AC15; Sigma), BrdU (Sigma), cofilin (38), Exp6 (ProteinTech), Flag (Sigma), histone H3 (Sigma), Ipo9 (Abnova), mCherry (Clonetech), and tubulin (Sigma). The secondary antibodies used in this study were: HRP conjugated anti-mouse, anti-rabbit, anti-HA, and anti-Flag (Sigma) and Alexa Fluor conjugated anti-mouse and anti-rabbit (Molecular Probes).

5-FUrd Incorporation. About 2,500 NIH 3T3 cells or Flag cell lines were seeded in 24-well plates on 13 mm coverslips (Thermo Scientific) overnight. Cells were transfected with 10 nM siRNAs as described in *Supporting Information*, and after the second transfection incubated for 4 d. For the rescue, cells were transfected with 100 ng RNAi-resistant Ipo9-cherry DNA construct, using lipofectamine transfection reagent (Invitrogen) according to the manufacturer. On day 5 of RNAi, a control siRNA treated coverslip was exposed to actinomycin D for 3 hr before media for all wells was changed to fresh media containing 2 mM 5-FUrd (Sigma). Cells were incubated for 20 min in 5-FUrd, fixed, and permeabilized as described below. Cells were blocked with 5% BSA for 1 h and stained with 1:250 dilution of rabbit anti-Flag and/or mouse anti-BrdU in PBS. After 1 h, coverslips were washed with PBS and counter stained with Alexa Fluor-dye conjugated anti-rabbit and/or anti-mouse and DAPI (Sigma). Coverslips were mounted and images were acquired as described below. The intensity of 5-FUrd in the nuclei was quantified using ImageJ. The data were normalized to the median value of the control sample for each staining to exclude the variation in antibody dilutions between individual experiments.

Immunofluorescence and Microscopy. Cells (both NIH 3T3 and S2R+) were fixed with 4% paraformaldehyde (PFA) in PBS for 20 min, washed with PBS, and permeabilized using 0.1% Triton-X 100 (Sigma) in PBS. Cover slips were washed with PBS, and when applicable stained with Alexa Fluor 594-conjugated phalloidin (Molecular Probes) and DAPI for 30 min. After staining, coverslips were washed with PBS and mounted using Moviol 1,4-diazabicyclo [2,2,2] octane (Sigma). Images of fixed cells were either acquired using the Olympus AX70 microscope equipped with the F-view II camera and analySIS software (Olympus) or Axio Imager M2 with AxioCam HRm camera and AxioVision software (Zeiss) using 63x/1.4 objective. Confocal images were acquired with Leica TCS SP5 confocal microscope, 63x/1.3 objective and LAS AF software. Where applicable, nuclear and cytoplasmic intensities were quantified using either imageJ or LAS AF Lite (Leica). In such cases, equal areas of both nucleus and cytoplasm of each cell, representing more than half the entire nuclear area, are measured and the ratio is calculated by dividing the average nuclear intensity by the average cytoplasmic intensity. Data are then normalized to the respective control samples.

Cell Fractionation. Cells were fractionated to nuclear and cytoplasmic fractions using the ProteoJET nuclear cytoplasmic proteins separation kit (Fermentas). The concentrations were determined using the Bradford method and the same amount of protein was loaded into each well (1 μg). Nuclear and cytoplasmic proteins were separated in 12% SDS polyacrylamide electro-

phoretic gels, transferred onto nitrocellulose membrane, and the level of actin was detected with antiactin AC-15. Antihistone H3 and antitubulin were used both as loading controls and to ensure that the fractionation had worked. Bands were quantified using the Quantity One software (BioRad). The actin bands were first normalized against the respective loading control (tubulin for cytoplasmic fractions and histone H3 for nuclear fractions) and then to total actin, which did not significantly vary between the different conditions.

Immunoprecipitation. For immunoprecipitation (IP), 1.5×10^6 NIH 3T3 cells were seeded on 15 cm plates and transfected the next day with 4 μg of 2Flag-actin/2Flag-cofilin/empty Flag vector and with 6 μg of 2HA-Ipo9. After 48 h cells were lysed by using the ProteoJET kit (Fermentas), and cell lysates diluted 1:2 with 50 mM Tris·HCl (pH 7.5), 100 mM NaCl, and Protease Inhibitor Cocktail (Roche) (IP-buffer). After clearing the lysate, 30 μL of anti-Flag M2 affinity gel was added to the lysates, and when indicated supplemented with 50 μM of Ran-Q69L, which was expressed and purified as described before (Izaurralde et al., 1997). After 3 h on rotation at +4 °C, the samples were washed three times with IP-buffer, and bound proteins eluted with 80 μL of 1 x SDS/PAGE loading buffer, which did not contain any reducing reagents. For depletion of cofilin, the cleared cell lysate was first incubated with 1 μg of anticofilin-1 antibody (38) for 1 h on rotation at +4 °C. Then 30 μL of Protein A-sepharose was added, and the sample incubated for 2 h. The supernatant was then used for the IP with the Flag-affinity gel as above. Samples (20% of the immunoprecipitates and 5% of the inputs) were separated in 12% SDS/PAGE, transferred onto nitrocellulose membrane and the immunoprecipitated proteins detected with directly conjugated anti-Flag M2-peroxidase, anti-HA HA-7 peroxidase, or with rabbit anticofilin (38)

Microinjection. For microinjection, NIH 3T3 cells were seeded and treated as described for the 5-FUrd incorporation. Dextrans of 40 kDa and 70 kDa labeled with FITC (Invitrogen) and Alexa Fluor 488 labeled rabbit muscle actin (Invitrogen) were injected in concentrations of approximately 1–3 mg/mL in G-buffer using Eppendorf Femtotips. Injection pressure (pi) was 250–350 hPa and injection time 0.4–0.6 s. Fresh media was changed on cells intended for live-cell imaging, and they were analyzed within 2–24 h after delivering the fluorescent dye.

Live-Cell Imaging. NIH 3T3 cells were grown on 35 mm dishes and imaged in 37°C under a CO_2 hood. Leica TCS SP5 laser scanning confocal microscope equipped with 270 mW optically pumped semiconductor laser at 90% hardware power was used for the imaging. LAS AF version used was 2.4.1 build 6384, and data were collected in 12-bit format. GFP, Alexa Fluor 488, and FITC were excited at 488 nm and detected at 511 nm. All fluorophores were imaged with a 0.9 NA HCX APO L 63x objective at 0.5% software laser power whereas 100% software power and "zoom in"—function was used for bleaching. To minimize any contaminating cytoplasmic signal, pinhole = 1 was used and the z-axis level was carefully chosen approximately in the middle of the nucleus using nuclear envelope and nucleoli as points of focus.

Export FLIP assay. The purpose of this assay is to continuously photobleach the cytoplasm excluding the nucleus and thereby impose a situation where the loss of nuclear fluorescence can be used as a measure of export of fluorescent particles from the nucleus to the cytoplasm, where they are subsequently photolytically quenched. Due to repeated bleaching there will be negligible reimport of fluorescent molecules that would attenuate the loss of fluorescence from the nucleus. LAS AF "Live data mode" was used to design a cycle ("pattern") suitable for measuring nuclear export. After the acquisition of two prebleach frames, the microscope was instructed to bleach the whole cytoplasm after which a postbleach picture was taken. This 3 × bleach + 1 × image cycle was repeated 50 times taking approximately 5 min. The region of interest (ROI) covering the cytoplasm was carefully drawn to avoid any nuclear overlap and a minimum distance of approximately 1 μm from nuclear envelope was kept. Images were obtained using 256 × 256 resolution, 700 Hz and line average 2. For analysis, background was subtracted and prebleach nuclear signal intensity was set to one. Data represent two to three independent experiments.

Import FRAP assay. In this assay the whole nuclear volume is bleached and the subsequent reappearance of nuclear fluorescence represents the immediate import of unbleached fluorescent molecules from the cytoplasm. Because single-photon laser will also bleach a portion of cytoplasm residing below and above the nucleus, continuous bleaching cannot be used to measure import. For both import assays, LAS AF FRAP Wizard was utilized. In general, first two prebleach frames were taken, then the nucleus was bleached with one to two frames and fluorescence recovery measured for a short (1 min) or long (40 min) time. In the short assay, pictures were taken with a resolution of 256 × 256, 700 Hz, line average 2. Settings were the same in the longer assay except 1,024 × 1,024 resolution was used. For analysis, background was subtracted and data were normalized to prebleach (=1) and bleaching (=0) nuclear signal intensities. Data represent two to three independent experiments.

The longer FRAP curves for GFP-actin and GFP-actin-R62D were analyzed in Origin (7.5) by using one to three component exponential analysis. The recovery curves for GFP-actin are best fit with a triple exponential equation ($y = y0 + A1 * (1 - \exp(-x/t1)) + A2 * (1 - \exp(-x/t2)) + A3 * (1 - \exp(-x/t3))$), with fitted parameters $y0 = 0.22 +/- 0.006$, $A1 = 0.47 +/- 0.012$, $t1 = 1800 +/- 300$, $A2 = 0.11 +/- 0.007$, $t2 = 6.8 +/- 0.9$, $A3 = 0.19 +/- 0.022$, and $t3 = 230 +/- 32$. The parameters for double exponential fit were $y0 = 0.27 +/- 0.005$, $A1 = 0.15 +/- 0.008$, $t1 = 55 +/- 6.9$, $A2 = 0.50 +/- 0.006$, $t2 = 1040 +/- 48$. The goodness of fit increased from double to triple exponential analysis (double exponential $Chi^2/DoF = 0.00016$, $R^2 = 0.99545$ and triple exponential $Chi^2/DoF = 0.00006$, $R^2 = 0.99819$), and also inspection of the residuals confirmed this notion. The recovery curves for GFP-actin-R62D were best fit with a double exponential equation ($y = y0 + A1 * (1 - \exp(-x/t1)) + A2 * (1 - \exp(-x/t2))$), with fitted parameters of $y0 = 0.48 +/- 0.010$, $A1 = 0.17 +/- 0.010$, $t1 = 4.5 +/- 0.5$, $A2 = 0.28 +/- 0.004$, and $t2 = 330 +/- 11$. For R62D, the goodness of fit did not improve from double to triple exponential analysis ($Chi^2/DoF = 0.00014$, $R^2 = 0.98872$ for both triple and double exponentials), and in triple exponential analysis, the second and third halftimes were in practice identical.

Statistical Analyses. Statistical analyses were performed in Excel or Sigma Plot 11.0. The data for nuclear/cytoplasm fluorescence intensities, actin-R62D distribution and actin levels in nucleus from Western blots were analyzed by two-tailed students t-test because the data conformed to normal distribution. Significance was determined by $P < 0.05$, and the actual P values are indicated in figure legends. Data from 5 FUrd incorporation were analyzed with a Mann–Whitney rank sum test, and the significance determined by $P < 0.001$. SigmaPlot does not report the actual P values for this particular test.

ACKNOWLEDGMENTS. We thank Pekka Lappalainen and members of the Vartiainen and Lappalainen laboratories for critical reading of the manuscript. Microinjection was performed at the Department of Biosciences with assistance from Esa Kuismanen. Imaging was performed at the Light Microscopy Unit, Institute of Biotechnology. M.K.V. is funded by the Academy of Finland, University of Helsinki research funds, and Sigrid Juselius Foundation. J.D. is funded by a fellowship from the Helsinki Graduate Program in Biotechnology and Molecular Biology, and K.-P.S. by a fellowship from the Viikki Graduate School in Biosciences.

1. Misteli T (2007) Beyond the sequence: Cellular organization of genome function. *Cell* 128:787–800.
2. Zhao K, et al. (1998) Rapid and phosphoinositol-dependent binding of the SWI/SNF-like BAF complex to chromatin after T lymphocyte receptor signaling. *Cell* 95:625–636.
3. Farrants AK (2008) Chromatin remodelling and actin organisation. *FEBS Lett* 582:2041–2050.
4. Hofmann WA, et al. (2004) Actin is part of pre-initiation complexes and is necessary for transcription by RNA polymerase II. *Nat Cell Biol* 6:1094–1101.
5. Philimonenko VV, et al. (2004) Nuclear actin and myosin I are required for RNA polymerase I transcription. *Nat Cell Biol* 6:1165–1172.
6. Hu P, Wu S, Hernandez N (2004) A role for beta-actin in RNA polymerase III transcription. *Genes Dev* 18:3010–3015.
7. Obrdlik A, et al. (2008) The histone acetyltransferase PCAF associates with actin and hnRNP U for RNA polymerase II transcription. *Mol Cell Biol* 28:6342–6357.
8. Kukalev A, Nord Y, Palmberg C, Bergman T, Percipalle P (2005) Actin and hnRNP U cooperate for productive transcription by RNA polymerase II. *Nat Struct Mol Biol* 12:238–244.
9. Percipalle P, et al. (2002) Nuclear actin is associated with a specific subset of hnRNP A/B-type proteins. *Nucleic Acids Res* 30:1725–1734.
10. Vartiainen MK, Guettler S, Larijani B, Treisman R (2007) Nuclear actin regulates dynamic subcellular localization and activity of the SRF cofactor MAL. *Science* 316:1749–1752.
11. Huang W, et al. (2011) Coronin 2A mediates actin-dependent de-repression of inflammatory response genes. *Nature* 470:414–418.
12. Pollard TD, Borisy GG (2003) Cellular motility driven by assembly and disassembly of actin filaments. *Cell* 112:453–465.
13. Sweeney HL, Houdusse A (2010) Structural and functional insights into the myosin motor mechanism. *Annu Rev Biophys* 39:539–557.

14. Chuang CH, et al. (2006) Long-range directional movement of an interphase chromosome site. *Curr Biol* 16:825–831.
15. Hu Q, et al. (2008) Enhancing nuclear receptor-induced transcription requires nuclear motor and LSD1-dependent gene networking in interchromatin granules. *Proc Natl Acad Sci USA* 105:19199–19204.
16. Dundr M, et al. (2007) Actin-dependent intranuclear repositioning of an active gene locus in vivo. *J Cell Biol* 179:1095–1103.
17. Mehta IS, Amira M, Harvey AJ, Bridger JM (2010) Rapid chromosome territory relocation by nuclear motor activity in response to serum removal in primary human fibroblasts. *Genome Biol* 11:R5.
18. Pederson T, Aebi U (2005) Nuclear actin extends, with no contraction in sight. *Mol Biol Cell* 16:5055–5060.
19. Vartiainen MK (2008) Nuclear actin dynamics—from form to function. *FEBS Lett* 582:2033–2040.
20. McDonald D, Carrero G, Andrin C, de Vries G, Hendzel MJ (2006) Nucleoplasmic beta-actin exists in a dynamic equilibrium between low-mobility polymeric species and rapidly diffusing populations. *J Cell Biol* 172:541–552.
21. Miyamoto K, Pasque V, Jullien J, Gurdon JB (2011) Nuclear actin polymerization is required for transcriptional reprogramming of Oct4 by oocytes. *Genes Dev* 25:946–958.
22. Spencer VA, et al. (2011) Depletion of nuclear actin is a key mediator of quiescence in epithelial cells. *J Cell Sci* 124:123–132.
23. Xu YZ, Thuraisingam T, Morais DA, Rola-Pleszczynski M, Radzioch D (2010) Nuclear translocation of beta-actin is involved in transcriptional regulation during macrophage differentiation of HL-60 cells. *Mol Biol Cell* 21:811–820.
24. Bohnsack MT, Stuven T, Kuhn C, Cordes VC, Gorlich D (2006) A selective block of nuclear actin export stabilizes the giant nuclei of Xenopus oocytes. *Nat Cell Biol* 8:257–263.
25. Fornerod M, Ohno M, Yoshida M, Mattaj IW (1997) CRM1 is an export receptor for leucine-rich nuclear export signals. *Cell* 90:1051–1060.
26. Wada A, Fukuda M, Mishima M, Nishida E (1998) Nuclear export of actin: a novel mechanism regulating the subcellular localization of a major cytoskeletal protein. *EMBO J* 17:1635–1641.
27. Stuven T, Hartmann E, Gorlich D (2003) Exportin 6: A novel nuclear export receptor that is specific for profilin.actin complexes. *EMBO J* 22:5928–5940.
28. Terry LJ, Shows EB, Wente SR (2007) Crossing the nuclear envelope: Hierarchical regulation of nucleocytoplasmic transport. *Science* 318:1412–1416.
29. Keminer O, Peters R (1999) Permeability of single nuclear pores. *Biophys J* 77:217–228.
30. Paine PL, Moore LC, Horowitz SB (1975) Nuclear envelope permeability. *Nature* 254:109–114.
31. Barden JA, Tulloch PA, dos Remedios CG (1981) Crystalline actin tubes. IV. Structural information on actin monomers obtained from computer-averaged lattice images. *J Biochem* 90:287–290.
32. Posern G, Sotiropoulos A, Treisman R (2002) Mutant actins demonstrate a role for unpolymerized actin in control of transcription by serum response factor. *Mol Biol Cell* 13:4167–4178.
33. Park SH, Park TJ, Lim IK (2011) Reduction of exportin 6 activity leads to actin accumulation via failure of RanGTP restoration and NTF2 sequestration in the nuclei of senescent cells. *Exp Cell Res* 317:941–954.
34. Rohn JL, et al. (2011) Comparative RNAi screening identifies a conserved core metazoan actinome by phenotype. *J Cell Biol* 194:789–805.
35. Pendleton A, Pope B, Weeds A, Koffer A (2003) Latrunculin B or ATP depletion induces cofilin-dependent translocation of actin into nuclei of mast cells. *J Biol Chem* 278:14394–14400.
36. Niwa R, Nagata-Ohashi K, Takeichi M, Mizuno K, Uemura T (2002) Control of actin reorganization by Slingshot, a family of phosphatases that dephosphorylate ADF/cofilin. *Cell* 108:233–246.
37. Vartiainen MK, et al. (2002) The three mouse actin-depolymerizing factor/cofilins evolved to fulfill cell-type-specific requirements for actin dynamics. *Mol Biol Cell* 13:183–194.
38. Hotulainen P, Paunola E, Vartiainen MK, Lappalainen P (2005) Actin-depolymerizing factor and cofilin-1 play overlapping roles in promoting rapid F-actin depolymerization in mammalian nonmuscle cells. *Mol Biol Cell* 16:649–664.
39. Lappalainen P, Drubin DG (1997) Cofilin promotes rapid actin filament turnover in vivo. *Nature* 388:78–82.
40. Bischoff FR, Klebe C, Kretschmer J, Wittinghofer A, Ponstingl H (1994) RanGAP1 induces GTPase activity of nuclear Ras-related Ran. *Proc Natl Acad Sci USA* 91:2587–2591.
41. Gorlich D, Pante N, Kutay U, Aebi U, Bischoff FR (1996) Identification of different roles for RanGDP and RanGTP in nuclear protein import. *EMBO J* 15:5584–5594.
42. Obrdlik A, Percipalle P (2011) The F-actin severing protein cofilin-1 is required for RNA polymerase II transcription elongation. *Nucleus* 2:72–79.
43. Hofmann WA, et al. (2009) SUMOylation of nuclear actin. *J Cell Biol* 186:193–200.
44. Fomproix N, Percipalle P (2004) An actin-myosin complex on actively transcribing genes. *Exp Cell Res* 294:140–148.
45. Muhlhausser P, Muller EC, Otto A, Kutay U (2001) Multiple pathways contribute to nuclear import of core histones. *EMBO Rep* 2:690–696.
46. Waldmann I, Walde S, Kehlenbach RH (2007) Nuclear import of c-Jun is mediated by multiple transport receptors. *J Biol Chem* 282:27685–27692.
47. Filion GJ, et al. (2010) Systematic protein location mapping reveals five principal chromatin types in Drosophila cells. *Cell* 143:212–224.